Desalination and Water Treatment
www.deswater.com

doi: 10.5004/dwt.2022.28149

252 (2022) 140–147
March

Electrochemical sensor based on EDTA functionalized carbon nanotubes for anodic stripping determination of lead ions

Jingying Ma[a], Xiaoping Hong[b,*]

[a]*Department of Construction, Zhejiang College of Construction, Hangzhou 311231, China, email: majy75@163.com*
[b]*Department of Chemistry, Zhejiang Sci-Tech University, Hangzhou 310028, China, email: xpnghong@sina.com*

Received 24 August 2021; Accepted 31 December 2021

ABSTRACT

A new electrochemical sensor for the determination of lead ions was fabricated by modifying glassy carbon electrode (GCE) with novel laboratory-produced nanomaterials synthesized by the silanization reaction between N-[(3-trimethoxysilyl) propyl] ethylenediamine triacetic acid trisodium (NTMP-EDTA) and hydroxyl functionalized multi-walled carbon nanotubes (MWCNTs-OH). The synergistic effect of the carbon nanotubes (CNTs) and EDTA groups anchored on the surface of CNTs resulted in improved sensor performance toward the detection of trace lead ions. Under the optimal conditions, the anodic stripping currents of the sensor varied linearly with the concentration of lead ions from 2.0 to 470 μg/L, with the detection limit estimated to 0.7 μg/L. The sensor was also successfully used for the analysis of trace lead ions in real samples with good accuracy, sensitivity, selectivity, and recovery.

Keywords: Carbon nanotubes; EDTA functional; Silanization; Lead ions

1. Introduction

Soil and natural water systems are at increased risk from heavy metal pollution originated from mining production, metal processing, and the power battery industry. Heavy metal ions including lead (Pb^{2+}), cadmium (Cd^{2+}), and chromium (VI) are highly toxic and can cause irreversible and severe damage to human health, such as kidney damage, liver injury, brain disorders, and carcinogenic risk [1]. Therefore, preventing environmental pollution from heavy metals is a challenging task. Various analytical techniques, such as spectrophotometric methods [2], atomic absorption spectrometry (AAS) [3, 4], inductively coupled plasma (ICP) method [5], and X-ray fluorescence (XRF) [6] have been used for the detection of trace heavy metal ions. However, these techniques are time-consuming, expensive, less sensitive, and limited in terms of real-time applications [7].

Alternatively, electrochemical techniques have been used to detect trace amounts of heavy metals in food, soil, wastewater, and natural water samples attributing to their excellent features such as simple operation, low cost, quick response, facile miniaturization, and convenience of *in-situ* application [8,9]. Although electrochemical methods are efficient for sensing heavy metals, they still suffer from low sensitivity, selectivity, and poor stability [10]. Hence, the fabrication of highly sensitive, cost-effective, facile, and highly selective electrochemical devices for the detection of heavy metal pollutions is highly desirable.

Advanced materials, such as nanocarbon materials [11,12], noble metal nanoparticles [13-15], metal oxide nanoparticles [16,17], as well as composite materials containing two or more types of nanomaterials [18,19] have been investigated as electrode modifiers to promote the performances of modified electrodes owing to their high specific surface areas, good catalytic effects, and unique conductivities. Carbon nanotubes (CNTs) are representative nanomaterials that have been utilized as ideal electrode materials owing to their super conductivities, high specific surface

* Corresponding author.

areas, superior electrocatalytic effects, and antifouling performances [20]. So far, numerous sensors based on carbon nanotubes have been developed for sensing trace organic or inorganic molecules [21,22]. However, the hydrophobicity of pristine CNTs creates a thermodynamic barrier of enriching trace heavy metal ions onto the surface of CNTs [23]. This issue has been solved by functionalization of the surface of CNTs by hydroxylation or carboxylation and anchoring their surface to improve affinity between heavy metal ions and CNT fibers.

Ethylenediaminetetraacetic acid (EDTA) disodium salt possesses four carboxylic groups and two nitrogen atoms, which can strongly coordinate with alkaline earth or transition-metal ions by chelating reactions. As a result, EDTA is often used as a chelating agent for heavy metal removal from waters or soils.

In this article, a new functional CNT material was modified on a glassy carbon electrode and used as a sensor for the determination of heavy metal ions. To improve the affinity toward heavy metal ions, N-[(3-trimethoxysilyl) propyl] ethylenediamine triacetic acid (NTMP-EDTA) trisodium salt was used as a functional molecule for linking to the surface of CNTs through silanization reaction. The obtained EDTA functionalized CNTs (CNT-EDTA) were then used to fabricate chemically modified electrodes for detection of specific heavy metal ions. The strategy of the whole experimental procedure is illustrated in Fig. 1. Positive lead ions can be electrically attracted by the cathodic CNT-EDTA modified electrode and captured to form stable Pb^{2+}-EDTA complex by the EDTA groups anchored on the surface of CNTs. After a cathodic pretreatment and a following anodic stripping procedure, sensitive stripping current responses were recorded for the analysis of trace lead ions.

2. Experimental

2.1. Materials

Hydroxyl functionalized multi-walled carbon nanotubes (MWCNT-OH) were purchased from Jicang Nano (China) and used as received without further pretreatment. NTMP-EDTA solution (40%) was obtained from Fluorochem Ltd., (Derbyshire, UK). Analytical grade lead nitrate was supplied by Energy Chemical, China. All other analytical grade chemicals were purchased from Chinese Chemical, China. Deionized water was prepared using an Academic Millipore system (Millipore Inc., MA, USA) and used in all the experiments.

2.2. Apparatus

Electrochemical characterizations were carried out using a CHI660B (Chenhua Instrument, Shanghai, China) electroanalytical workstation equipped with a three-electrode system. Glassy carbon electrodes (GCEs) and a series of chemical modified GCEs were used as the working electrodes. A platinum wire was used as an auxiliary electrode and AgCl/Ag electrode (support electrolyte: saturated potassium chloride solution) was utilized as a reference. The morphologies of CNTs were investigated by field-emission scanning electron microscopy (FE-SEM) (Hitachi S-4800, Tokyo, Japan). Infrared spectra of MWCNT-OH before and after the silanization reaction were recorded using a Fourier transform infra-red (FT-IR) spectrometer (Nicolet 5700, Wisconsin, USA).

2.3. Preparation of EDTA functional multi-walled carbon nanotubes (MWCNT-EDTA)

MWCNT-EDTA was synthesized following literature method [24]. Briefly, 150 mL methanol or 150 mL ethanol was first added into a three-neck flask as a supporting solvent. Next, 100.0 mg MWCNT-OH was added to the flask and agitated thoroughly in an ultrasonic bath for 30 min. Afterward, 3.0 mL NTMP-EDTA (40%) was injected into the flask and stirred consecutively at 60°C–65°C for 10 h. After the completion of the silanization reaction, the obtained black mixture was filtered under vacuum using a 0.22 μm PTFE membrane. The resulting filter cake was rinsed thoroughly with deionized water three times. After removal of impurities, the black filter cake was dried in a vacuum oven at 60°C for 24 h. Finally, the black dried product was ground thoroughly in an agate mortar to obtain a homogeneously black powder, denoted as MWCNT-EDTA.

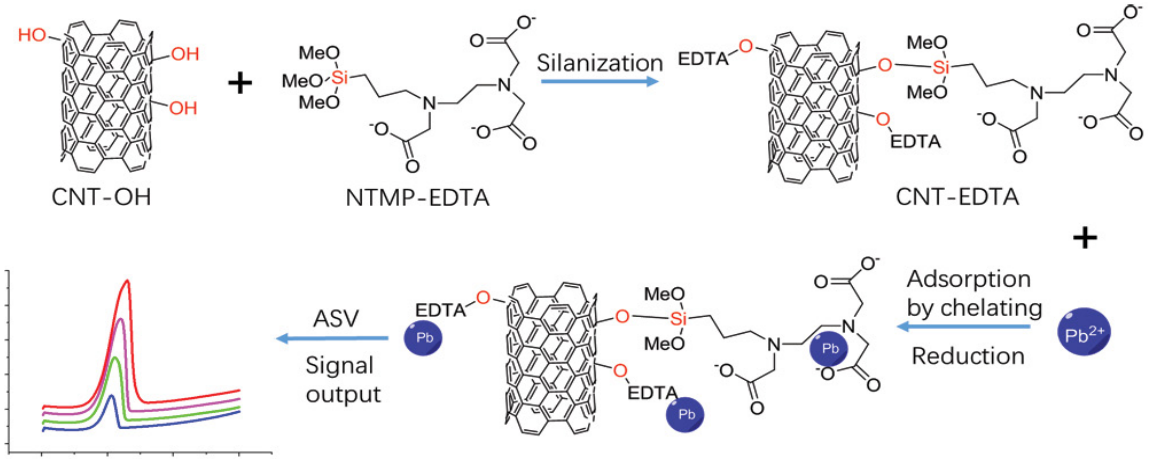

Fig. 1. Overview of the preparation process of CNT-EDTA and its application.

2.4. Fabrication of modified electrodes

MWCNT-EDTA powder (5 mg) was weighed and dispersed in 5.0 mL deionized water under sonication to obtain a homogeneous black gel. Glassy carbon electrode (GCE) was used as the substruction electrodes. Before the use, the GCE was polished with 0.05 μm alumina particles followed by cleaning. Several milliliters of MWCNT-EDTA gel were then cast onto the clean GCE surface using a syringe. The evaporation of the solvent under ambient conditions afforded MWCNT-EDTA modified electrode (MWCNT-EDTA-GCE). Another MWCNT-OH modified electrode (MWCNT-OH-GCE) was prepared for comparison using the same mentioned-above procedure.

3. Results and discussion

3.1. Effect of EDTA functionalization

MWCNT-OH and MWCNT-EDTA materials were characterized by various analytical techniques. The morphologies of the nanomaterials before and after the silanization reaction were investigated by SEM. As shown in Fig. 2a, the MWCNT-OH fibers looked disordered and tightly entangled. By comparison, the MWCNT-EDTA nanofibers are ordered and loose (Fig. 2b). This difference was probably induced by the hydrophilic characteristic and electrostatic repulsive force of the carboxyl groups introduced on the surface of CNTs after the silanization reaction.

The FT-IR spectra of MWCNT-OH (blue curve) and EDTA functionalized MWCNTs under ethanol (red curve) and methanol (green curve) as the silanization reaction solvents are compared as shown in Fig. 2c. The typical absorption signals at approximately 3,450 and 1,630 cm^{-1} attributed to the stretching of the O–H anchored on the MNCNTs and the C=C stretching of the framework of MWCNTs, respectively. New absorption peaks at approximately 2,923 cm^{-1} ($–CH_2–$ stretching), 1,720 cm^{-1} (C=O stretching), and 1,390 cm^{-1} (C–O stretching) in red and blue curves were observed corresponding to the methylene groups and carboxyl groups of EDTA linked to the surface of MWCNTs as a result of the silanization reaction. Accordingly, EDTA-modified MWCNTs were successfully synthesized. However, the absorption peak at 2,923 cm^{-1} in the red curve was stronger than that in the blue curve. Thus, the silanization reactions of NTMP-EDTA and MWCNTs-OH were more effective in ethanol than in methanol.

The adsorption ability of MWCNT-EDTA toward Pb^{2+} in the presence of diphenyl sulfide hydrazone (DSH) solution as the indicator agent is shown in Fig. 2d. 10 mL deionized water was taken in a glass vial, followed by adding 5 drops of DSH indicator, immediately resulting in a homogeneous pale yellow solution (Fig. 2dA). Next, the solution turned pink after the injection of 1.0 mL Pb^{2+} solution (1.0 mg/mL) into the vial (Fig. 2dB), indicating the color of the complex of Pb^{2+} and DSH indicator. Afterward, 10 mg MWCNT-OH was dropped into the

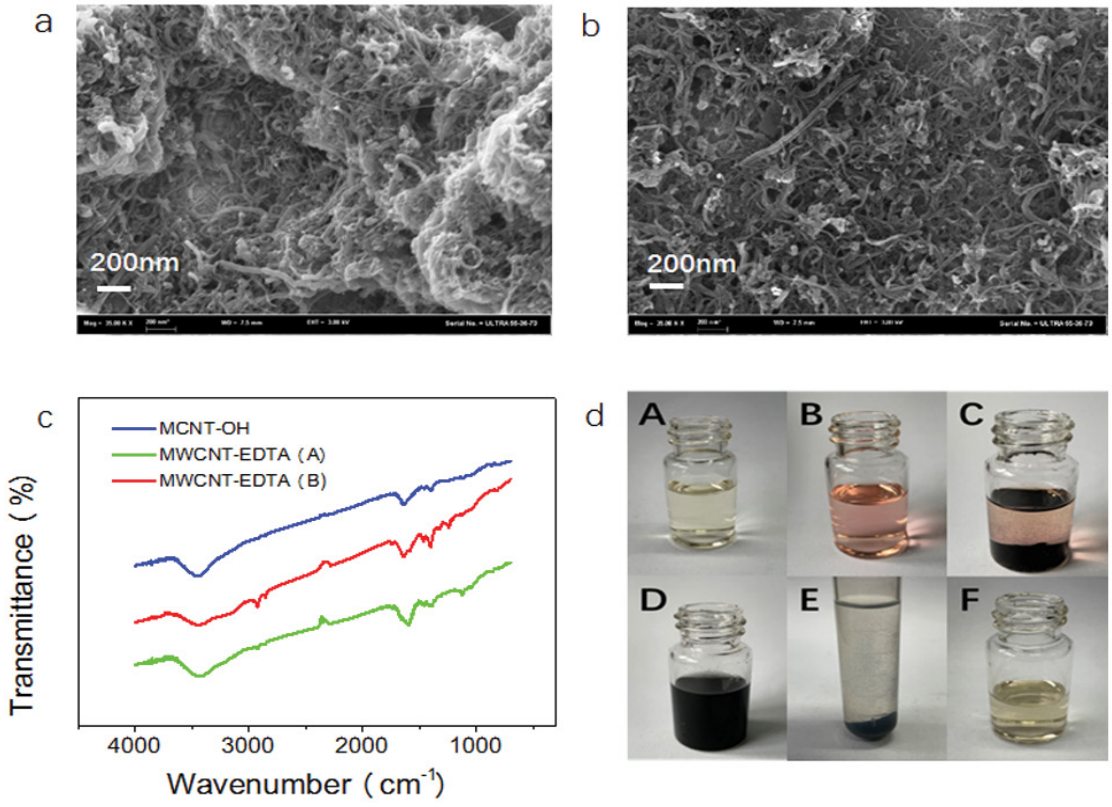

Fig. 2. Characterization of MWCNT-EDTA: (a) SEM morphology of MWCNT-OH, (b) SEM morphology of MWCNT-EDTA, (c) FT-IR spectra of MWCNT-OH and MWCNT-EDTA, and (d) Pb^{2+} ions adsorption performance of MWCNT-EDTA.

vial as a lead adsorbent (Fig. 2dC). After 2 h of sedimentation, the supernatant still kept a weak pink color, suggesting remained lead ions in the solution. Another 10 mL of deionized water was also added to a newly cleaned vial. After the injection of 1.0 mL Pb^{2+} solution (1.0 mg/mL) into the vial, 10 mg MWCNT-EDTA was dropped into the vial and violently agitated in the same ultrasonic bath for 5 min (Fig. 2dD). After standing for 10 min, the black dispersion system was centrifuged for 3 min at 3,000 rpm (Fig. 2dE). Next, 5 mL of the supernatant was transferred to a newly cleaned vial. The solution then turned to yellow (the color of the indicator) after adding 5 drops of DSH indicator into the vial (Fig. 2dF), suggesting that Pb^{2+} was completely adsorbed onto the as-prepared MWCNT-EDTA.

3.2. Electrochemical properties of MWCNT-EDTA modified electrodes

Several unmodified and modified GCEs were prepared by the above-mentioned procedure. Electrochemical impedance spectroscopy (EIS) was used to investigate the interfacial properties of the electrodes before and after the modification. EIS Nyquist plots were recorded at an applied potential of 0.22 V, 5 mV amplitude, and frequencies from 0.1 to 10^5 Hz in 0.2 M KCl electrolyte containing 2.5 mM potassium ferricyanide and potassium ferrocyanide as the probe. MWCNT-OH-GCE and MWCNT-EDTA-GCE were used as the working electrodes. Under the same experimental conditions (Fig. 3a), the pristine GCE showed the biggest semicircle diameter (curve a), corresponding to the charge transfer resistance (R_{ct}) at high frequencies. Hence, the pristine GCE demonstrated the highest electron transfer resistance. However, the electron transfer resistance significantly decreased when the GC electrode was modified with MWCNT-OH (curve b) or MWCNT-EDTA (curve c), probably attributing to the high conductivity of MWCNTs. In addition, the MWCNT-EDTA modified electrode exhibited the lowest electron transfer resistance owning to the excellent hydrophilicity of MWCNT-EDTA that enhanced the coating of the EDTA functionalized nanomaterial layer onto the surface of the GC electrode tightly.

The stripping current responses of Pb^{2+} (0.5 mg/L) in pH 5.2 buffer containing sodium acetate and acetic acid as the supporting electrolytes are illustrated in Fig. 3b. After 2 min cathodic potential (–0.8 V) preconcentration procedure, square wave voltammetry (SWV) anodic stripping was applied on GCE (black curve), MWCNT-OH-GCE (green curve), and MWCNT-EDTA-GCE (red curve) working electrodes (Fig. 3b). A weak current response was observed at approximately –0.58 V (black curve) when GCE was used as the working electrode. In addition, a distinct current peak (green curve) was observed for MWCNT-OH-GCE. Surprisingly, a sharp current peak (red curve) about two folds of that obtained by a MWCNT-OH-GCE was monitored when a MWCNT-EDTA-GCE was used as the working electrode. The sensitive electrochemical response of MWCNT-EDTA-GCE toward trace lead ions probably attributed to the synergistic effect of CNT and the EDTA groups functionalization, resulting in active surface area of the modified electrode increasing, electrostatic attraction between lead ions and carboxyl groups and strong chelating ability of EDTA groups anchored on the surface of CNTs.

3.3. Optimization of electrochemical procedure

The solution pH used during the SWV anodic stripping of lead ions is a key factor in performance as the chelation ability of the EDTA groups anchored on the surface of the MWCNTs is related to pH of the solution. Higher pH values would lead to modified electrodes with strong capacity. As shown in Fig. 4a, the increase in the pH value of the supporting electrolytes promoted the stripping currents sharply, suggesting MWCNT-EDTA-GCE with superior enrichment capacity toward lead ions. However, the stripping currents turned to passivation at pH > 5.2, probably because of the hydrolysis of lead ions and precipitation under weakly acidic or neutral conditions.

Different modified electrodes were prepared by casting 2, 4, 6, and 7 μL MWCNT-EDTA gel onto the surfaces of cleaned GCEs. As shown in Fig. 4b, the stripping currents steadily promoted and leveled off after exceeding 6 μL modifier. Another key factor affecting the current response of the modified electrode is the cathodic potential during the lead ions enrichment procedure. As depicted in Fig. 4c, lower enrichment potentials induced higher stripping currents. Finally, the stripping currents leveled off at a cathodic potential <–0.8 V.

The effect of cathodic treatment time is displayed in Fig. 4d, indicating that the stripping current increased steadily with treatment time. A passivation platform of

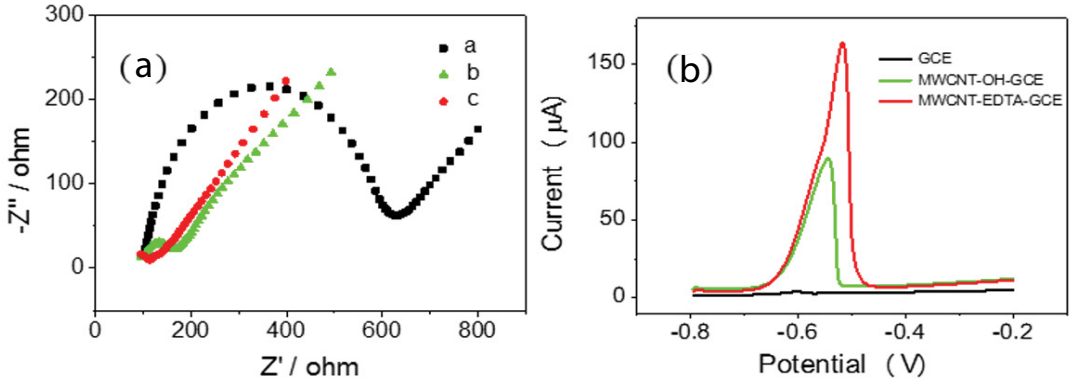

Fig. 3. AC impedance (a) and square wave voltammetry (b) characterization of obtained electrodes.

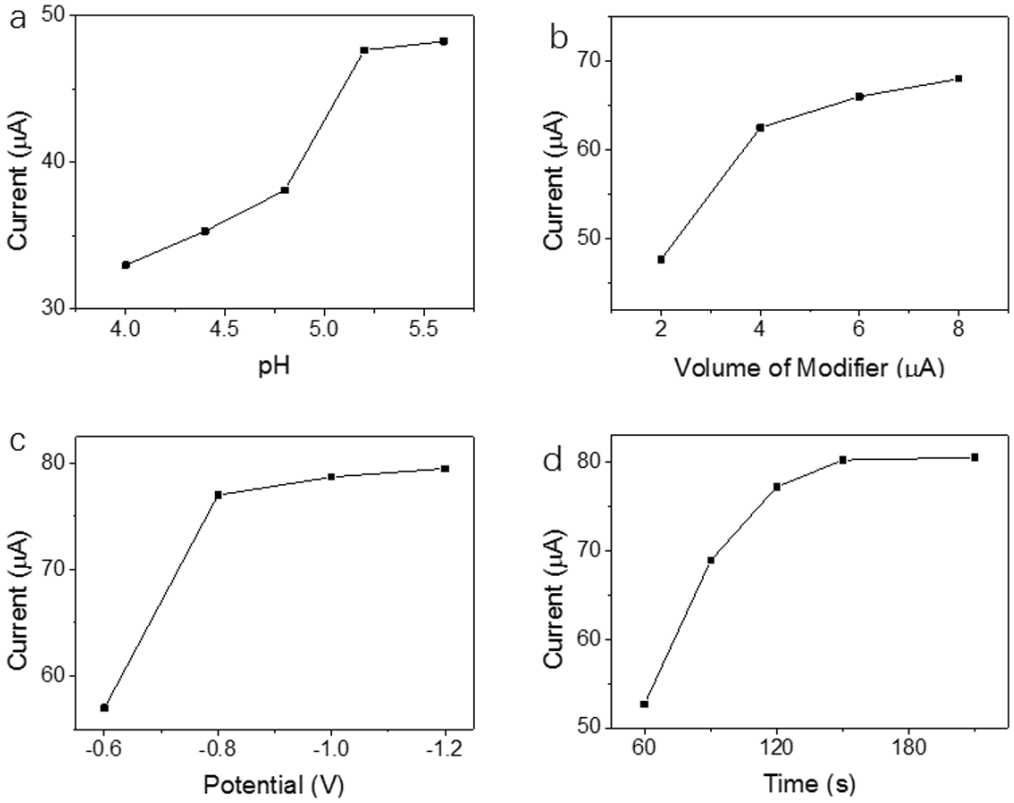

Fig. 4. Influencing factors on the responses of modified electrodes. (a) Anodic stripping current response of lead ions in electrolytes of different pH values. (b) Interference of modifier dosage. Effect of (c) cathodic potential during lead preconcentration and (d) cathodic reaction time.

striping current was obtained at treatment time exceeding 120 s. In sum, the optimal working conditions were identified as pH of 5.2, modifier dosage of 6 μL, cathodic potential of –0.8 V, and enrichment time of 120 s.

3.4. Detection of lead ions

The concentration of lead ions was determined by SWV anodic stripping method under the above-mentioned optimized parameters. Several lead ions solutions were produced by diluting the stock solution. As illustrated in Fig. 5a, the stripping peak at approximately –0.58 V increased steadily with increasing lead ions concentration. Besides, the anodic stripping current varied linearly with the lead concentration from 2.0 to 470 μg/L (Fig. 5b) with a correlation equation determined as: $I(\mu A) = 0.387 \times C + 0.672$ (coefficient $R^2 = 0.993$). The detection limit was estimated as 0.6 μg/L, and calculated according to $3S_b/k$ [25], where k represents the slope of the calibration plot and S_b is the average noise response obtained in a blank solution. The stability of the modified electrodes was evaluated by successively applying SWV anodic stripping in lead ions solution at C = 200 μg/L for 10 d. After each anodic stripping test, the modified electrode was stored under a cleaned atmosphere. After 10 d, the current response maintained almost 97% of its original value (Fig. 5c), indicating satisfactory stability (RSD = 0.91%). Besides, six MWCNT-EDTA-GCEs produced with the same procedure were also subjected to striping tests in the same lead solution, and the reproducibility was estimated to 11.2%. The interference of co-existing metal ions during lead ions determination was also evaluated. A pH 5.2 solution containing 0.5 mg Cu^{2+}, Pb^{2+}, and Cd^{2+} was prepared for the stripping experiments. Fig. 5d shows three completely separated anodic peaks with the lead peak showing an outstanding intensity between those of Cu and Cd peaks. Hence, the interference of Cu and Cd could be ignored.

The analytical performances of the produced modified electrodes were also compared with those of similar published sensors. As listed in Table 1, the analytical performances of the proposed sensor in terms of LOD and linear range were superior to those of traditional flame atomic absorption spectrometry (FL-AAS) and similar to those of graphite furnace atomic absorption spectrometry (GF-AAS). Compared to recently reported electrochemical methods, the MWCNT-EDTA-GCE illustrated a similar LOD, but markedly wider linear detection range. Hence, the proposed modified electrode looks more convenient for practical applications.

3.5. Application in real samples

To investigate the applicability of the as-prepared modified electrodes, MWCNT-EDTA-GCE was used for the determination of lead ions in real samples. To this end, water samples from an unnamed lake in Zhejiang Sci-Tech

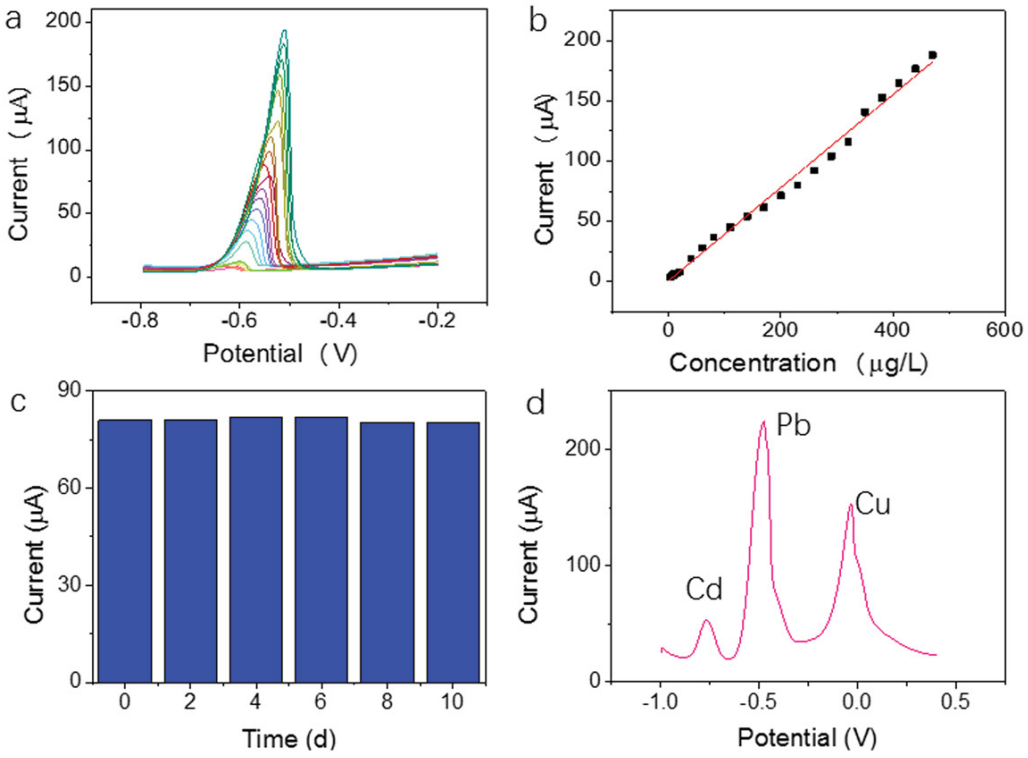

Fig. 5. Performance of MWCNT-EDTA-GCE toward lead ions detection. (a) SWV stripping response of lead solution with different concentrations. (b) Calibration plot of stripping currents vs. lead concentration. (c) Stability of MWCNT-EDTA-GCE during continuous testing. (d) Interference of co-existing heavy metal ions.

Table 1
Comparison of the analytical performances of sensors reported in the literature and this work

Method	LOD	Linear range	Reference
FL-AAS	0.17 mg/L	0.5–250 mg/L	[26]
GF-AAS	0.25 μg/L	1.0–8.0 μg/L	[27]
ND-BC-CTS/GCE	0.056 μmol/L	0.25–6.0 μmol/L	[28]
SWCNH sensor	0.4 μg/L	1.0–60.0 μg/L	[29]
PA/PPy/GO ME	0.41 μg/L	5–150 μg/L	[30]
PDAN-MSPD	0.3 μg/L	0.5–5.0 μg/L	[31]
MWCNTs-COOH/UiO-66-NH_2/MWCNTs-COOH/GCE	0.0771 ppb	1–121 ppb	[32]
B/P-OMCs/GCE	1.5 μg/L	2.07–248 μg/L	[33]
Co-N_x-C@MWCNTs	0.7 μg/L	2–60 μg/L	[34]
PySA/GCE	0.007 μg/L	–	[35]
This work	0.6 μg/L	2.0–470 μg/L	–

ND-BC-CTS/GCE: nanodiamonds-biochar-chitosan/GCE, SWCNH: single-walled carbon nanohorns, PA/PPy/GO ME: phytic acid/polypyrrole/graphene oxide modified electrode, PDAN-MSPD: poly(1,5-diaminonaphthalene)-modified screen-printed device, UiO-66-NH_2: Zr-metal-organic frameworks, B/P-OMCs: B/P-doped ordered mesoporous carbons, Co-N_x-C@MWCNTs: cobalt centered bimetallic framework, and PySA/GCE: pyridine-2-sulfonic acid/GCE.

University were first pretreated by filtration to remove insoluble substances. Next, the pH of the samples was carefully controlled at 5.2 using a stock sodium acetate and acetic acid buffer. The levels of lead ions in the samples before and after the addition of lead standard stock solution were then monitored by MWCNT-EDTA-GCE and graphite furnace atomic absorption spectrometry (GF-AAS). As listed in Table 2, the as-prepared modified electrode exhibited similar detection accuracy and recovery as those of GF-AAS.

4. Conclusions

In summary, EDTA functionalized MWCNTs were successfully prepared through a mild and facile silanization

Table 2
Application of MWCNT-EDTA-GCE in real samples

Sample	Spiked (μg/L)	Found (μg/L)		Recovery (%)	
		Sensor	GF-AAS	Sensor	GF-AAS
1	0	0	0	–	–
2	20.0	18.1	19.1	90.5	95.5
3	200	193	192	96.5	96.0

reaction with NTMP-EDTA as the silanizing agent. Attributing to the unique chelating ability of EDTA groups and high specific surface area of MWCNTs, the EDTA functionalized MWCNTs exhibited outstanding adsorption capacity toward heavy metal ions. Accordingly, the new functional material was also successfully applied for the fabrication of highly sensitive and stable modified electrodes toward the detection of lead ions. The resulting electrodes inherited the attractive properties of MWCNTs with the unique chelating ability of EDTA functional groups, ensuring good accuracy, high sensitivity, and satisfying selectivity toward the detection of trace lead ions in water samples.

Acknowledgments

This work was financially supported by the Science and Technology Plan Project of Zhejiang Province (Grant No. 2020C03087) and the Scientific Research Fund of Zhejiang College of Construction (Grant No. Z202002).

References

[1] V. Kumar, R.D. Parihar, A. Sharma, P. Bakshi, G.P.S. Sidhu, A.S. Bali, L. Karaouzas, R. Bhardwaj, A.K. Thukral, Y. Gyasi-Agyei, J. Rodrigo-Comino, Global evaluation of heavy metal content in surface water bodies: a meta-analysis using heavy metal pollution indices and multivariate statistical analyses, Chemosphere, 236 (2019) 124364, doi: 10.1016/j.chemosphere.2019.124364.

[2] Y. Guo, C. Teng, J. Liu, X. Liu, X. Bian, Q. Zhang, Spectrophotometric determination of trace heavy metal ions in water with the assistance of electrospun nanofiber membrane extraction and chemometrics calculation, J. Appl. Spectrosc., 87 (2020) 174–179.

[3] I. Menezes, P.D. Nascimento, M.H. Gonzalez, A. Oliveira, Simple and robust GFAAS methods for determination of As, Cd, and Pb in hemp products using different sample preparation strategies, Food Anal. Methods, 14 (2021) 1043–1053.

[4] L.J. Huang, W. Huang, R.J. Shen, Q. Shuai, Chitosan/thiol functionalized metal–organic framework composite for the simultaneous determination of lead and cadmium ions in food samples, Food Chem., 330 (2020) 127212, doi: 10.1016/j.foodchem.2020.127212.

[5] L.L. Zhao, S.X. Zhong, K.M. Fang, Z.S. Qian, J.R. Chen, Determination of cadmium(II), cobalt(II), nickel(II), lead(II), zinc(II), and copper(II) in water samples using dual-cloud point extraction and inductively coupled plasma emission spectrometry, J. Hazard. Mater., 239 (2012) 206–212.

[6] E. Haque, P.S. Thorne, A.A. Nghiem, C.S. Yip, B.C. Bostick, Lead (Pb) concentrations and speciation in residential soils from an urban community impacted by multiple legacy sources, J. Hazard. Mater., 416 (2021) 125886, doi: 10.1016/j.jhazmat.2021.125886.

[7] M. Malakootian, H. Abolghasemi, H. Mahmoudi-Moghaddam, A novel electrochemical sensor based on the modified carbon paste using Eu^{3+} – doped NiO for simultaneous determination of Pb(II) and Cd(II), J. Electroanal. Chem., 876 (2020) 114474, doi: 10.1016/j.jelechem.2020.114474.

[8] F.A. Gutierrez, J.M. Gonzalez-Dominguez, A. Ansón-Casaos, J. Hernández-Ferrer, M.D. Rubianes, M.T. Martínez, G. Rivas, Single-walled carbon nanotubes covalently functionalized with cysteine: a new alternative for the highly sensitive and selective Cd(II) quantification, Sens. Actuators, B, 249 (2017) 506–514.

[9] C. Fan, L. Chen, R. Jiang, J. Ye, H. Li, Y. Shi, Y. Luo, G. Wang, J. Hou, X. Guo, $ZnFe_2O_4$ nanoparticles for electrochemical determination of trace Hg(II), Pb(II), Cu(II), and glucose, ACS Appl. Nano Mater., 4 (2021) 4026–4036.

[10] M. Li, H.L. Gou, I. Al-Ogaidi, N.Q. Wu, Nanostructured sensors for detection of heavy metals: a review, ACS Sustainable Chem. Eng., 1 (2013) 713–723.

[11] N. Baig, M. Sajid, T.A. Saleh, Recent trends in nanomaterial-modified electrodes for electroanalytical applications, TrAC, Trends Anal. Chem., 111 (2019) 47–61.

[12] B.Y.G. Pan, L. Bai, C.M. Hu, X.P. Wang, W.S. Li, F.G. Zhao, Graphene-indanthrone donor-π-acceptor heterojunctions for high-performance flexible supercapacitors, Adv. Energy Mater., 10 (2020) 202000181, doi: 10.1002/aenm.202000181.

[13] L. Wang, J. Li, Y.F. Pan, L.F. Min, Y.C. Zhang, X.Y. Hu, Z.J. Yang, Platinum nanoparticle-assembled nanoflake-like tin disulfide for enzyme-based amperometric sensing of glucose, Microchem. Acta, 184 (2017) 2357–2363.

[14] H. Karimi-Maleh, K. Cellat, K. Arikan, A. Savk, F. Karimi, F. Sen, Palladium–nickel nanoparticles decorated on functionalized-MWCNT for high precision non-enzymatic glucose sensing, Mater. Chem. Phys., 250 (2020) 123042, doi: 10.1016/j.matchemphys.2020.123042.

[15] Y.M. Leng, K. Jiang, W.T. Zhang, Y.H. Wang, Synthesis of gold nanoparticles from Au(I) ions that shuttle to solidify: application on the sensor array design, Langmuir, 33 (2017) 6398–6403.

[16] J.N. Baby, B. Sriram, S.F. Wang, M. George, Effect of various deep eutectic solvents on the sustainable synthesis of $MgFe_2O_4$ nanoparticles for simultaneous electrochemical determination of nitrofurantoin and 4-nitrophenol, ACS Sustainable Chem. Eng., 8 (2020) 1479–1486.

[17] M.M. Alam, A.M. Asiri, M.T. Uddin, M.A. Islam, M.R. Awual, M.M. Rahman, Detection of uric acid based on doped ZnO/Ag_2O/Co_3O_4 nanoparticle loaded glassy carbon electrode, New J. Chem., 43 (2019) 8651–8659.

[18] Q.G. He, J. Liu, X.P. Liu, G.L. Li, D.C. Chen, P.H. Deng, J. Liang, A promising sensing platform toward dopamine using MnO_2 nanowires/electro-reduced graphene oxide composites, Electrochim. Acta, 296 (2019) 683–692.

[19] H. Bagheri, A. Hajian, M. Rezaei, A. Shirzadmehr, Composite of Cu metal nanoparticles-multiwall carbon nanotubes-reduced graphene oxide as a novel and high performance platform of the electrochemical sensor for simultaneous determination of nitrite and nitrate, J. Hazard. Mater., 324 (2017) 762–772.

[20] R.T. Kachoosangi, M.M. Musameh, I. Abu-Yousef, J.M. Yousef, S.M. Kanan, L. Xiao, S.G. Davies, A. Russell, R.G. Compton, Carbon nanotube-ionic liquid composite sensors and biosensors, Anal. Chem., 81 (2009) 435–442.

[21] J.C. Hu, Z.G. Zhang, Application of electrochemical sensors based on carbon nanomaterials for detection of flavonoids, Nanomaterials, 10 (2020) 10102020, doi: 10.3390/nano10102020.

[22] H.L. Yang, W.T. Xu, X.Y. Liang, Y.Y. Yang, Y. Zhou, Carbon nanotubes in electrochemical, colorimetric, and fluorimetric immunosensors and immunoassays: a review, Microchim. Acta, 187 (2020), doi: 10.1007/s00604-020-4172-4.

[23] L. Jin-Hyon, P. Ungyu, Dispersion stability of single-walled carbon nanotubes using Nafion in biosolvent, J. Phys. Chem. C, 111 (2007) 2477–2483.

[24] S. Hou, S. Su, M.L. Kasner, P. Shah, K. Patel, C.J. Madarang, Formation of highly stable dispersions of silane-functionalized reduced graphene oxide, Chem. Phys. Lett., 501 (2010) 68–74.

[25] K. Hasebe, J. Osteryoung, Differential pulse polarographic determination of some carcinogenic nitrosamines, Anal. Chem., 47 (1975) 2412–2418.

[26] N. Altunay, A. Elik, D. Bingol, Simple and green heat-induced deep eutectic solvent microextraction for determination of lead

and cadmium in vegetable samples by flame atomic absorption spectrometry: a multivariate study, Biol. Trace Elem. Res., 198 (2020) 324–331.
[27] S. Bakirdere, T. Yaroglu, N. Tirik, M. Demiroz, A.K. Fidan, O. Maruldali, A. Karaca, Determination of As, Cd, and Pb in tap water and bottled water samples by using optimized GFAAS system with Pd-Mg and Ni as matrix modifiers, J. Spectrosc., 2013 (2013) 824817, doi: 10.1155/2013/824817.
[28] A. Wong, P.A. Ferreira, A.M. Santos, F.H. Cincotto, R.A.B. Silva, M. Sotomayor, A new electrochemical sensor based on eco-friendly chemistry for the simultaneous determination of toxic trace elements, Microchem. J., 158 (2020) 105292, doi: 10.1016/j.microc.2020.105292.
[29] Y. Yao, H. Wu, J.F. Ping, Simultaneous determination of Cd(II) and Pb(II) ions in honey and milk samples using a single-walled carbon nanohorns modified screen-printed electrochemical sensor, Food Chem., 274 (2019) 8–15.
[30] H. Dai, N. Wang, D. Wang, H. Ma, M. Lin, An electrochemical sensor based on phytic acid functionalized polypyrrole/graphene oxide nanocomposites for simultaneous determination of Cd(II) and Pb(II), Chem. Eng. J., 299 (2016) 150–155.
[31] M.T.T. Nguyen, H.L. Nguyen, D.T. Nguyen, Poly(1,5-Diaminonaphthalene)-modified screen-printed device for electrochemical lead ion sensing, Adv. Polym. Technol., 2021 (2021) 6637316, doi: 10.1155/2021/6637316.
[32] Z. Lu, W. Zhao, L. Wu, J. He, W. Dai, C. Zhou, H. Du, J. Ye, Tunable electrochemical of electrosynthesized layer-by-layer multilayer films based on multi-walled carbon nanotubes and metal-organic framework as high-performance electrochemical sensor for simultaneous determination cadmium and lead, Sens. Actuators, B, 326 (2021) 128957, doi: 10.1016/j.snb.2020.128957.
[33] Y.-L. Xie, Sensitive determination of lead(II), copper(II), and mercury(II) based on B/P-doped ordered mesoporous carbons, Int. J. Electrochem. Sci., (2020) 12339–12352.
[34] R. Zhao, X.X. Wu, Y.X. Gao, Y.N. Liu, J.J. Gao, Y.M. Chen, Z. Zheng, W. Gan, Q.H. Yuan, A unique bimetallic MOF derived carbon-MWCNTs hybrid structure for selective electrochemical determination of lead ion in aqueous solution, Microchem. J., 158 (2020) 105271, doi: 10.1016/j.microc.2020.105271.
[35] H. Xiao, W. Wang, S. Pi, Y. Cheng, Q. Xie, Pyridine-2-sulfonic (or carboxylic) acid modified glassy carbon electrode for anodic stripping voltammetry analysis of Cd^{2+} and Pb^{2}, Anal. Chim. Acta, 1135 (2020) 20–28.